JOURNAL OF EXPERIMENTAL AND THEORETICAL PHYSICS, 2024, Vol. 165, No. 3, pp. 367–373

SOLID BODIES AND LIQUIDS

CHARACTERISTICS OF DEFECTS AND ENTROPY OF MIXING IN HIGH-ENTROPY ALLOYS OF THE FeNiCrCoCu SYSTEM

© 2024 R.A. Konchakov[a*], A.S. Makarov[a], N.P. Kobelev[b], V.A. Khonik[b]

[a] Department of General Physics, State Pedagogical University, 394043, Voronezh, Russia

[b] Institute of Solid State Physics, Russian Academy of Sciences, 142432, Chernogolovka, Moscow region, Russia

*e-mail: konchakov.roman@gmail.com

Received July 17, 2023

Revised October 03, 2023

Accepted November 06, 2023

Abstract. Classical molecular dynamics simulation for a number of single crystals of FeNiCrCoCu system showed that with increasing entropy of mixing the average formation enthalpy of interstitial defects and their shear susceptibility decreases monotonically. For interstitial defects in crystals and defect subsystems of glasses of the same composition, has been established that the average deviator components of dipole tensors decrease with increasing entropy of mixing, and the decrease occurs more strongly in the high-entropy region. All this may indicate the presence of a correlation between mixing entropy and properties of the defect subsystem of crystalline and glassy states.

Keywords: *high-entropy alloys, mixing entropy, molecular dynamics, interstitial defects, metallic glasses*

DOI: 10.31857/S00444510240306e4

1. INTRODUCTION

Entropy is the most important thermodynamic potential characterizing the glassy state. This is primarily due to the use of alloys with high glass-forming capacity [1-5]. Interest in the entropy of glasses has increased significantly in the last two decades due to intensive research on high-entropy alloys (HEA) [6-10]. The widespread definition of the concept of "high-entropy alloy" is based on the calculation of the entropy of mixing

$$S_{mix} = -R\Sigma c_i \ln(c_i),$$

where c_i is the atomic concentrations of the alloy components, R is the gas constant [7, 10]. Alloys for which $S_{mix} > 1.5$. are considered to be highly entropic.

Crystalline HEA usually have a faceted cubic, hexagonal, or volume-centered cubic lattice [11-14]. HEA have specific mechanical, transport, electrical and magnetic properties [11, 15-17], their thermal properties are extremely sensitive to small changes in the entropy of laughter [18]. For example, a change in S_{mix} by a value of $0.02R$ leads to a significant (1.5-2-fold) change in the width of the supercooled liquid region and the melting interval [18]. The magnetic and magnetocaloric properties of high-entropy glasses of the GdScCoNiAl system are also very sensitive to changes in the entropy of mixing. In particular, a small change in S_{mix} leads to a significant change in magnetization, cell temperature, and magnetic entropy [18]. Thus, an important task is to clarify the role of entropy in the formation of HEA properties in crystalline and glassy states.

The main structural property of the glassy state is the presence of local ico-saedric symmetry [19-23]. At the same time, there are nanoscale regions in the stack that differ, in comparison with the surrounding amorphous matrix, in excess energy, reduced resistance to shear rearrangements and low-frequency features of the spectrum of vibrational density of states. Such areas are called glassy defects. Modern ideas about the structure and origin of defects in glasses are extremely diverse and widely discussed. For example, defects in glass are called free volume [24], shear transformation areas [25], flow defects [26], liquid-like areas [27], dynamic

inhomogeneities [28], areas of nonaffine displacements [29], string-like solitons [30], quasi-point defects [31], elastic dipoles [32].

The model of elastic dipoles seems attractive to us, as it allows us to compare the characteristics of defects in glass and the corresponding parent crystal, where these are interstitial defects in the dumbbell configuration [33], as well as to build a hypothesis about the origin of defects in glass. For example, in [34] a mechanism was proposed for the formation of an amorphous matrix and defects in amorphous aluminum based on the clustering of interstitial dumbbells arising during the melting of the crystal. As shown by the model calculation of the entropy of the formation of interstitial defects in aluminum, more than half of the excess entropy of the glassy state (the difference in the entropy of glass and the corresponding parent crystal) can be formed already at the melting stage due to the generation of interstitial dumbbells [35].

Based on the above, it can be assumed that a more detailed study of the subsystem of defects will be useful for understanding the properties of glasses, including high-entropy ones. The purpose of this work was to calculate the characteristics of defects in the crystalline and glassy states and to establish the correlation of these characteristics with the entropy of mixing S_{mix}. We are not aware of any similar studies.

2. SIMULATION TECHNIQUE

Alloys of the FeNiCrCoCu system were chosen for the study, since in the region of high-energy states (i.e. at $S_{mix} > 1.5$) the crystals of this system have a stable single-phase structure in the form of a deformed FCC lattice, which facilitates the calculation of elastic modulus. Calculations using the methods of classical molecular dynamics and statics were performed in the LAMMPS package [36] with an interatomic potential from the work [37]. We have previously used this potential to calculate the characteristics of defects in crystal $Fe_{20}Ni_{20}Cr_{20}Co_{20}Cu_{20}$ [38] and identify defects in glass of the same composition [33].

The composition of the model system varied as follows. The iron content increased in increments of 4 at.%, starting from the most highly entropic state with an equal content of components, and the content of all other components decreased by 1 at.%, respectively.

The initial crystal states were obtained by generating FCC lattices with a size of 4000 atoms (i.e. $10 \times 10 \times 10$ translations) with a random arrangement of atoms of different elements in appropriate proportions. The glassy states were created by quenching the melt from $T = 3000$ K to zero temperature with a cooling rate of $5 \cdot 10^{13}$ K/s.

The enthalpy of formation H_f of interstitial defects was calculated using the formula

$$H_f = H_{rel} - H_{ini}\frac{N \pm 1}{N},$$

where H_{ini} is the enthalpy of the ideal lattice, H_{rel} is the enthalpy of the system after the introduction of the defect and the relaxation of the structure. Interstitial defects in the dumbbell configuration were introduced into the system at $T = 0$ K with subsequent relaxation of the structure by the method of combined gradients.

The shear modulus was calculated at zero temperature as the ratio of the change in mechanical stresses to the corresponding small deformations of the model system. The shear susceptibility of the interstitial dumbbells in β was calculated using the le Granato shape [39]

$$G / G_{perf} = \exp(-\beta c),$$

where G_{perf} and G are the shear modules of a defect—free crystal and a crystal containing interstitial defects of a dumbbell configuration in concentration c, respectively.

The vibrational density of states (VDOS) spectra were calculated as the square of the Fourier transform module of the auto correlation function of velocity. At the same time, averaging of 100 vibrational spectra of VDOS was performed for each configuration of the model system.

The dipole tensor P_{ij} of elastic dipoles (interstitial defects) is defined as the derivative of the mechanical stress tensor σ_{ij} in terms of the number of n defects per unit volume at a constant strain value ε [40]:

$$P_{ij} = \frac{\partial \sigma_{ij}}{\partial n}\Big|_{\varepsilon}. \quad (1)$$

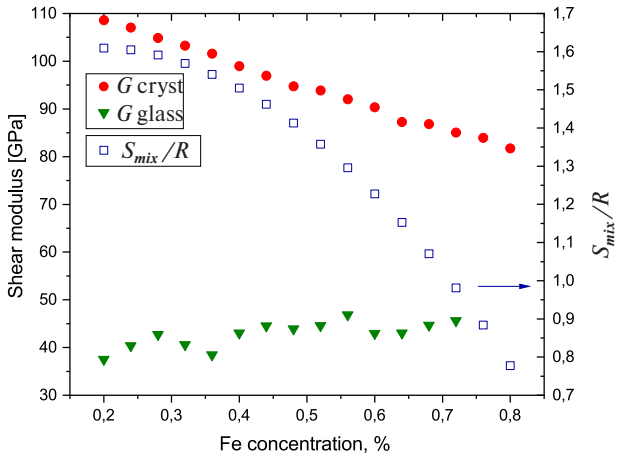

Fig. 1. Shear modulus of single crystals and glasses of the FeNiCrCoCu system (left scale) and entropy of mixing (right scale) depending on the concentration of iron in the alloy

In a computer model, the dipole tensors of defects can be calculated using an approximate formula [32, 33]

$$P_{ij} \approx V_0\left(\sigma_{ij}^{N+n_i} - \sigma_{ij}^{N}\right) / n^{int}, \qquad (2)$$

where N is the number of atoms in an ideal crystal lattice, n^{int} is the number of interstitial defects, V_0 is the volume of the model system.

In the case of glass, for which there is no generally accepted correct definition of a defect-free state, a dipole tensor was assigned to each atom of the model system

$$P_{ij} = V_0\left(\sigma_{ij}^{N} - \sigma_{ij}^{N-1}\right), \qquad (3)$$

where σ_{ij}^{N} and σ_{ij}^{N-1} are stress tensors before and after the removal of this atom [33]. Before the removal, the structure was optimized with a change in the volume of the model system. After removal, the structure was optimized without changing the volume, while maintaining $\varepsilon = \text{const}$, as required by the formula.

The calculated tensors P_{ij} were reduced to a diagonal form and represented as the sum of the spherical and deviatory components:

$$P_{ij} = \frac{1}{3}\delta_{ij}P_{ll} + \left(P_{ll} - \frac{1}{3}\delta_{ij}P_{ll}\right). \qquad (4)$$

The concentrations of defects in the glasses were estimated in two ways. The concentration of c_g was calculated on the basis of the interstitial theory [39] using the formula

$$c_g = -\frac{1}{\beta}\ln\frac{G_{glass}}{G_{cryst}},$$

where G_{glass} and G_{cryst} are the shear modules of the glass and the corresponding parent crystal. The concentration of c_d was calculated based on the analysis of the distribution of the maximum deviatory components of the dipole tensors of all glass atoms (described in more detail in the next section).

3. SIMULATION RESULTS AND DISCUSSION

Figure 1 shows the dependence of the shear modulus G of crystals and glasses on the concentration of iron in the alloy. The same figure shows the change in the mixing energy of S_{mix} with varying chemical composition. It can be seen that with a change in the chemical composition, the shear modulus of crystals decreases monotonously, with large values of the shear modulus being observed in the region of higher values. The glass shear modulus does not change so much, but on average it grows monotonously with increasing iron concentration.

Within the framework of the considered scheme of varying compositions, each alloy uniquely corresponds to a certain value of the entropy

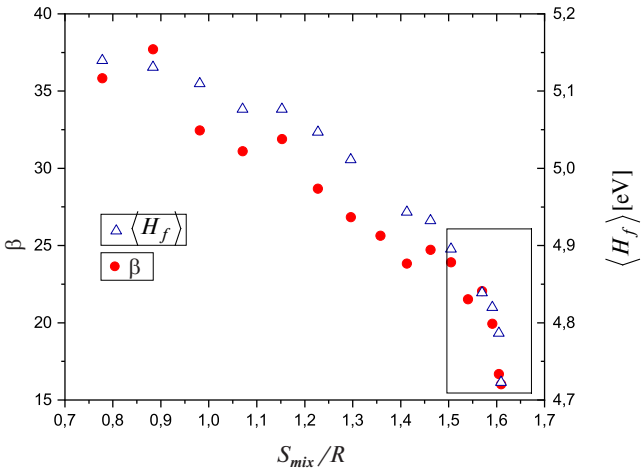

Fig. 2. The shear susceptibility of interstitial defects in single crystals of the FeNiCrCoCu system (left scale) and the average enthalpy of formation of interstitial defects (right scale) depending on the entropy of mixing

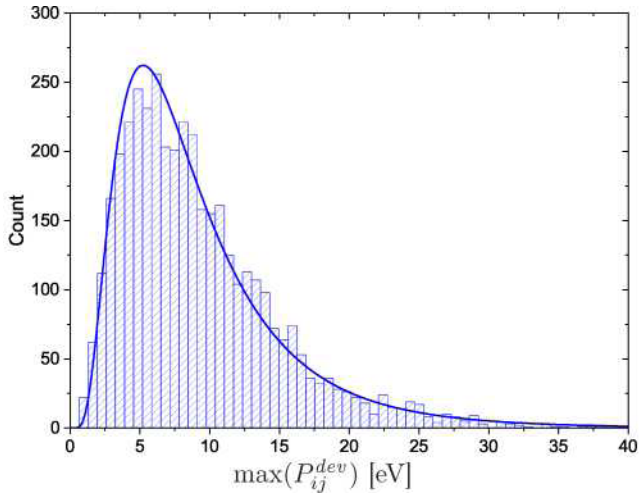

Fig. 3. Distribution of maximum deviatory components of dipole tensors of atoms in glass $Fe_{24}Ni_{19}Cr_{19}Co_{19}Cu_{19}$

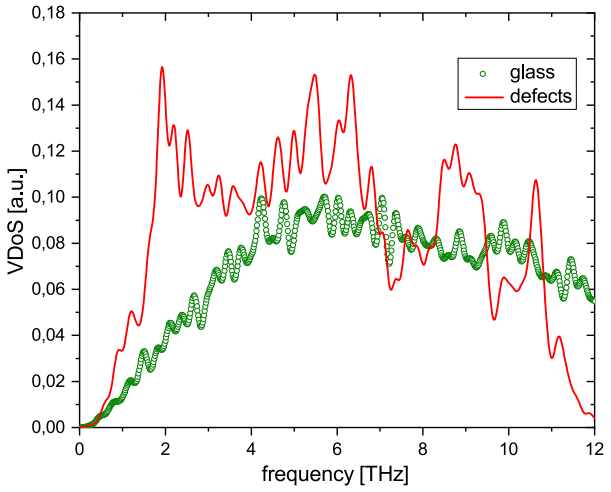

Fig. 4. Vibrational density spectra of $Fe_{24}Ni_{19}Cr_{19}Co_{19}Cu_{19}$ glass and its defect subsystems

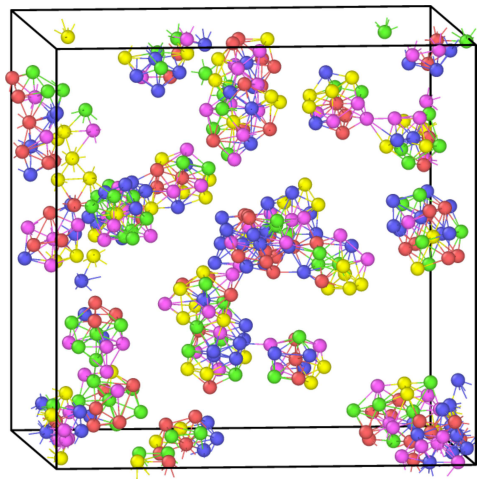

Fig. 5. Visualization of a part of the subsystem of defects with Voronoï indices ⟨0,1,10,2⟩ and ⟨0,2,8,2⟩ and their immediate environment in glass $Fe_{20}Ni_{20}Cr_{20}Co_{20}Cu_{20}$

of mixing S_{mix}. Therefore, it is possible to consider the dependence of various defect characteristics on the entropy of mixing as an independent parameter.

Figure 2 shows the dependence of the average enthalpy of formation of interstitial defects $\langle H_f \rangle$ on the entropy of mixing. It can be seen that in all cases the value $\langle H_f \rangle$ is quite high in comparison with that for individual components [41], i.e. alloys of the FeNiCrCoCu systems can have good radiation resistance. At the same time, a more intensive change in the enthalpy of formation of interstitial defects occurs in the range of high-energy states (at $S_{mix} > 1.5$), this region is divided by a rectangle.

The same Figure 2 shows the dependence of the shift susceptibility of interstitial defects β [39] on the entropy of mixing. It can be seen that the growth of S_{mix} leads to a monotonous change in shear susceptibility, which is an inter-lateral characteristic of interstitial defects. As in the case of $\langle H_f \rangle$, a stronger change in β occurs in the high-entropy region.

As mentioned above, structural defects in the glassy and crystalline states have a common microscopic nature — they are elastic dipoles. Therefore, it can be assumed that the value of S_{mix} will correlate with the properties of the subsystem of defects in glasses. The allocation of the subsystem of defects in glasses was carried out according to the scheme that was proposed by us in [33]. According to this scheme, the defect subsystem is formed by atoms in which the deviatory components of dipole tensors exceed the average value by 2.5 times. Figure 3 shows, for example, the distribution of the maximum deviatory components of the dipole tensors of atoms in glass $Fe_{24}Ni_{19}Cr_{19}Co_{19}Cu_{19}$. As in [33], this distribution has a form close to the lognormal distribution (shown by a solid curve).

As an indirect confirmation of the hypothesis that based on the analysis of dipole tensors can be identified, Fig. 4 shows the vibrational densities of the glass $Fe_{24}Ni_{19}Cr_{19}Co_{19}Cu_{19}$ and its defective subsystem. It can be seen that peaks characteristic of interstitial defects in crystals and defects in glasses are observed in the low frequency range (about 2 THz) [42-44].

Figure 5 shows, as an example, visualization using the OVITO program [45] of the distribution of atoms (and their nearest neighbors) forming part of the

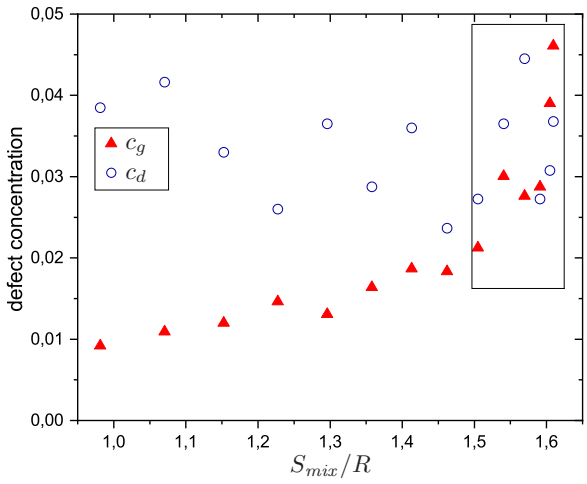

Fig. 6. Defect concentrations in glasses of the FeNiCrCoCu , system, calculated based on the analysis of deviatory components of dipole tensors [33], as well as on the basis of interstitial theory [39]

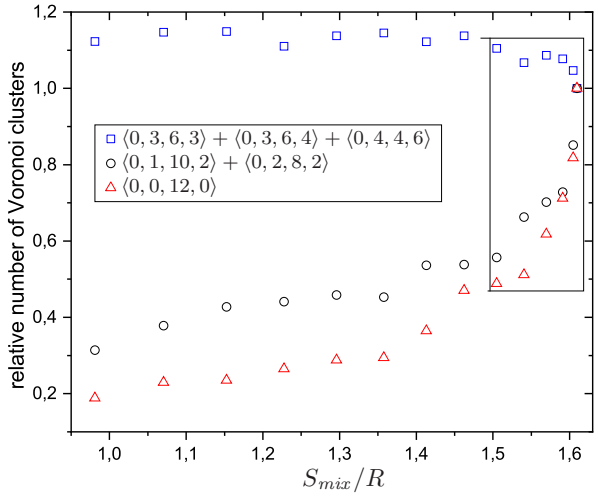

Fig. 7. The relative number of Voronoï polyhedra in glasses of the FeNiCrCoCu system depending on the entropy of mixing

subsystem of defects in glass $Fe_{20}Ni_{20}Cr_{20}Co_{20}Cu_{20}$, whose Voronoï indices are $\langle 0,1,10,2\rangle$ and $\langle 0,2,8,2\rangle$. It can be seen that the configuration of the defect subsystem is heterogeneous in the atomic environment.

Figure 6 shows a comparison of estimates of the concentration of defects c_g and c_d in glasses calculated on the basis of interstitial theory and from the analysis of distributions of deviatory components of dipole tensors, respectively. It can be seen that the values of the defect concentration in both cases are quite reasonable and are in good agreement, especially in the highly entropic region (highlighted by a rectangle).

As a structural characteristic of the studied systems, we used the distribution of Voronoï polyhedra, which are uniquely determined by a set of four indices $\langle n_3,n_4,n_5,n_6\rangle$. Figure 7 shows the relative number of the most common Voronoï polyhedral from entropy of mixing.

The number of corresponding polyhedra in the $Fe_{20}Ni_{20}Cr_{20}Co_{20}Cu_{20}$ system with the highest mixing entropy is taken as one. The same figure separately shows the relative number of icosahedral clusters with Voronoï indices $\langle 0,0,12,0\rangle$, which are of particular interest [20, 46].

Voronoï polyhedra with indices $\langle 0,1,10,2\rangle$ and $\langle 0,2,8,2\rangle$ are the most common among defects, their total concentration in glass is $Fe_{20}Ni_{20}Cr_{20}Co_{20}Cu_{20}$ about 0.6%. In turn, polyhedra with indices

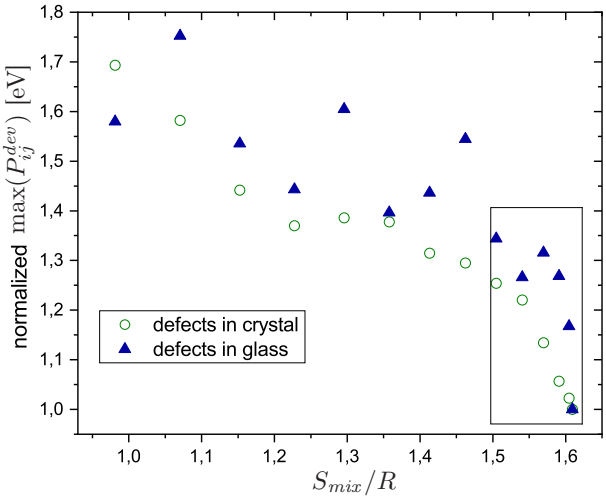

Fig. 8. Normalized average values of deviatory components of dipole tensors of defects in single crystals and glasses of the FeNiCrCoCu depending on the entropy of mixing.

$\langle 0,3,6,3\rangle$, $\langle 0,3,6,4\rangle$ and $\langle 0,4,4,6\rangle$ can be attributed to an amorphous matrix, since their total concentration in the most highly entropic glass is about 32%.

The concentration of icosahedral clusters in the same glass is about 0.5%. At the same time, the core of the icosahedral cluster consists of 13 atoms. If we add to them the atoms located in the first coordination sphere of the atoms of the nucleus, then the volume of the icosahedral cluster is about 45 atomic volumes. Next, we can estimate the volume fraction of these clusters (based on the 5% concentration of internodes, see Fig. 6), it turns out to be about 35%, which looks quite reasonable.

Figure 7 shows that, as in the case of shift susceptibility, a more dramatic change in the number of Voronoï polyhedra corresponding to defects and icosahedral clusters occurs in a highly entropic region highlighted by a rectangle.

Interstitial defects are elastic dipoles, and the magnitude of the deviatory components of the dipole tensors of elastic dipoles directly determines the degree of their interaction with the shear stress field. As was previously shown in [33] for $Fe_{20}Ni_{20}Cr_{20}Co_{20}Cu_{20}$ glass, the axes of elastic dipoles rotate during shear deformation of the model system. At the same time, the greatest angles of rotation are observed precisely in the area of the defect subsystem.

Figure 8 shows the dependences of the normalized average deviatory components of dipole tensors on the entropy of mixing for defects in monocrystals and glasses. The normalization was done for the values of the corresponding quantities in the state with the highest entropy of mixing (i.e., with equal concentrations of all components). It can be seen that with the growth of S_{mix} both values decrease. As for the previous defect characteristics, a more intensive reduction occurs in the high-entropy area highlighted by a rectangle.

A decrease in the average values of the deviatory components of dipole tensors may be a consequence of a decrease in the average enthalpy of defect formation, which contributes to the formation of a greater number of defects and a greater degree of their clustering. At the same time, clustering of defects of the interstitial type leads to a decrease in deviant components, which approach the values characteristic of an amorphous matrix [33].

4. CONCLUSION

For 16 metal alloys of the FeNiCrCoCu system, differing in the entropy of mixing, the average enthalpies of the formation of interstitial defects in the crystal, their shear susceptibilities and deviatory components of the dipolar tensors were calculated. It has been found that with an increase in the entropy of mixing, these characteristics decrease monotonously, while the decrease in the region of highly entropic states occurs faster.

For glasses of the same composition, the average deviatory components of the dipole tensors of the defect subsystem were calculated. It was found that with increasing entropy of mixing, these components, as in the crystal, decrease monotonously. Thus, it can be concluded that the characteristics of defects, both in crystalline and glassy states, correlate with the entropy of mixing.

The concentration of defects in glasses is estimated based on the analysis of the distributions of the deviator components of the dipole tensors of atoms. It is shown that in this case reasonable values of defect concentration are obtained, consistent with the corresponding estimates based on the interstitial theory.

The results obtained may be useful for understanding the role of mixing entropy in the formation of specific properties of high-energy alloys in crystalline and glass-like states.

FUNDING

The work was carried out with the support of the Russian Science Foundation (grant No. 23 12-00162).

REFERENCES

1. S. C. Glade, R. Busch, D. S. Lee, W. L. Johnson, J. Appl. Phys. 87, 7242–7248 (2000).

2. X. Ji, Y. Pan, J. Non-Cryst. Solids 353, 2443–2446 (2007).

3. S. Guo, Q. Hu, C. Ng, C. T. Liu, Intermetallics 41, 96-103 (2013).

4. H.-R. Jiang, B. Bochtler, S. S. Riegler, X.-S. Wei, N. Neuber, M. Frey, I. Gallino, R. Busch, J. Shen, J. Alloys Compd. 844, 156126 (2020).

5. A. S. Makarov, G. V. Afonin, R. A. Konchakov, V. A. Khonik, J. C. Qiao, A. N. Vasiliev, N. P. Kobelev, Scripta Mater. 239, 115783 (2024).

6. J. W. Yeh, S. K. Chen, S. J. Lin, J. Y. Gan, T. S. Chin, T. T. Shun, C. H. Tsau, S. Y. Chang, Adv. Eng. Mater. 6, 299 (2004).

7. E. P. George, D. Raabe, R. O. Ritchie, Nat. Rev. Mater. 4, 515 (2019).

8. Y. F. Ye, Q. Wang, J. Lu, C. T. Liu, Y. Yang, Materials Today 19, 349–362 (2016).

9. D. Kumar, Progress in Materials Science 136, 101106 (2023).

10. W. Chen, Nature Communications 14, 2856 (2023).

11. Y. Zhang, T. T. Zuo, Z. Tang, M. C. Gao, K. A. Dahmen, P. K. Liaw, Z. P. Lu, Progress in Materials Science 61, 1–93 (2014).

12. R. E. Ryltsev, S. Kh. Estemirova, V. S. Gaviko, D. A. Yagodin, V. A. Bykov, E. V. Sterkhov, L. A. Cherepanova, I. S. Sipatov, I. A. Balyakin, S. A. Uporov, Materialia 21, 101311 (2022).

13. S. Uporov, S. Kh. Estemirova, V. A. Bykov, D. A. Zamyatin, R. E. Ryltsev, Intermetallics 122, 106802 (2020).

14. S. A. Uporov, R. E. Ryltsev, S. Kh. Estemirova, E. V. Sterkhov, N. M. Chtchelkatchev, Scripta Materialia 193 108–111 (2021).

15. Z. Li, S. Zhao, R. O. Ritchie, M. A. Meyers, Progress in Materials Science 102, 296–345 (2019).

16. S. A. Uporov, R. E. Ryltsev, V. A. Bykov, S. Kh. Estemirova, D. . Zamyatin, Journal of Alloys and Compounds 820, 153228 (2020).

17. S. A.Uporov, R. E. Ryltsev, V. A. Sidorov, S. Kh Estemirova, E. V. Sterkhov, I. A. Balyakin, N. M. Chtchelkatchev, Intermetallics 140, 107394 (2022).

18. S. A. Uporov, R. E. Ryltsev, V. A. Bykov, N. S. Uporova, S. Kh Estemirova, N. M. Chtchelkatchev, Journal of Alloys and Compounds 854, 157170 (2021).

19. H .W. Sheng, W .K. Luo, F. M. Alamgir, E. Ma, Nature 439, 419 (2006).

20. Y. Q. Cheng, E. Ma, Prog. Mater. Sci. 56, 379 (2011).

21. W. H. Wang, Prog. Mater. Sci. 57, 487 (2012).

22. A. Hirata, P. Guan, T. Fujita, Y. Hirotsu, A. Inoue, A. R. Yavari, T. Sakurai, M. Chen, Nature Materials 10, 28-33 (2011).

23. A. Hirata, L. J. Kang, T. Fujita, B. Klumov, K. Matsue, M. Kotani, A. R. Yavari, M. W. Chen, Science 341, 376-379 (2013).

24. F. Spaepen, Acta Metall. 25, 407 (1977).

25. M. L. Falk, J. S. Langer, Phys. Rev. E 57, 7192 (1998).

26. Y. C. Hu, P. F. Guan, M. Z. Li, C. T. Liu, Y. Yang, H. Y. Bai, W. H. Wang, Phys. Rev. B 93, 214202 (2016).

27. T. Egami, S. J. Poon, Z. Zhang, V. Keppens, Phys. Rev. B 76, 024203 (2007).

28. M. D. Ediger, Annu. Rev. Phys. Chem. 51, 99128 (2000).

29. H. L. Peng, M. Z. Li, W. H. Wang, Phys. Rev. Lett. 106, 135503 (2011).

30. H. Zhang, C. Zhong, J. F. Douglas, X. Wang, Q. Cao, D. Zhang, J.-Z. Jiang, J. Chem. Phys. 142, 164506 (2015).

31. J. C. Qiao, J. M. Pelletier, J. Mater. Sci. Technol. 30, 523 (2014).

32. R. A. Konchakov, N. P. Kobelev, V. A. Khonik, A. S. Makarov, Physics of the Solid State 58(2), 215 (2016).

33. R. A. Konchakov, A. S. Makarov, A. S. Aronin, N. P. Kobelev, V. A. Khonik, JETP Letters 115(5), 280 (2022).

34. R. A. Konchakov, A. S. Makarov, N. P. Kobelev, A. M. Glezer, G. Wilde, V. A. Khonik, J. Phys.: Condens. Matter 31, 385703 (2019).

35. R. A. Konchakov, A. S. Makarov, A. S. Aronin, N. P. Kobelev, V. A. Khonik, JETP Letters 113, 345 (2021).

36. J. Plimpton, J. Comp. Phys. 117, 1 (1995).

37. D. Farkas, A. Caro, J. Mater. Res. 33, 3218 (2018).

38. M. A. Kretova, R. A. Konchakov, N. P. Kobelev, V. A. Khonik, JETP Letters 111(12), 679 (2020).

39. A. V. Granato, Eur. Phys. J. B 87, 18 (2014).

40. D. A. Freedman, D. Roundy, T. A. Arias1, Phys. Rev. B 80, 064108 (2009).

41. W.G. Wolfer, Fundamental properties of defects in metals, Comprehensive Nuclear Materials, ed. by R. J. M. Konings, Elsevier, Amsterdam (2012).

42. Y. Zhang, C. Z. Wang, F. Zhang, M. I. Mendelev, M. J. Kramer, K. M. Ho, Appl. Phys. Lett. 105, 151910 (2014).

43. T. Brink, L. Koch, K. Albe, Phys. Rev B 94, 224203 (2016).

44. N. P. Kobelev, V. A. Khonik, Physics–Uspekhi 193, 717 (2023).

45. B. A. Klumov, R. E. Ryltsev, N. M. Chtchelkatchev, JETP Letters 104, 546–551 (2016). 46. A. Stukowski, Modelling Simul. Mater. Sci. Eng. 18, 015012 (2010).